2018 REPORT – NSF RAPID - HURRICANE IRMA

What are the major goals of the project?

Recent exposure to a high-energy storm, Hurricane Irma (Sept 10, 2017), provided an opportunity to mobilize a research campaign to explicitly test a set of hypotheses to validate conceptual and computational models of how disturbance impacts and interactions among legacies influence ecosystem resilience. The project has three major goals associated with three hypotheses:

Goal 1 - Model Verification and Impact Assessment: Document the role of mangrove forests and elevation gradients in attenuating storm surge, and assess associated elevation changes driven by sediment deposits or losses. *Hypothesis*: Attenuation of Hurricane Irma storm surge by mangrove forests was greatest in areas that had gained elevation due to sediment delivery during Hurricane Wilma (2005), but erosive forces in the recent storm exceeded depositional in ways that will threaten resilience to saltwater encroachment.

Goal 2 - Fate and Flux of Nutrients and Carbon: Determine whether a storm surge erases or enhances a prior storm surge deposit, and influences the stability of mangrove-derived carbon in the coastal zone. *Hypothesis*: Hurricane Irma altered the inorganic carbon and phosphorus legacy deposited in the soil by Hurricane Wilma, and increased mobilization of previously stable organic carbon downstream and to the atmosphere, thereby decreasing resilience of the ecosystem to saltwater encroachment.

Goal 3 - Consumer Responses via Trophic Pathways and Distributional Shifts: Determine the influence of coastal storms on hydrologic connectivity and the access to food supplies by mobile consumers. *Hypothesis*: Large mobile consumers may have benefited from increased access to and quality of upstream food supplies during and after the storm due to a "browning" of the food web, and increased reliance on organic matter mobilized by the storm.

What was accomplished under these goals?

Major Activities

Goal 1 - Model Verification and Impact Assessment: We used a 2D Coastal and Estuarine Storm Tide (CEST) model to simulate Hurricane Irma's impact on South Florida and adjacent coastal areas (Table 1). The CEST model is discretized on an orthogonal curvilinear grid based on the modified C-grid with velocity components on the four edges of a grid cell and the water depths at the center and four edges (Zhang et al. 2013). The radiation open boundary condition was employed to allow waves to propagate out of the model domain (Blumberg and Kantha 1983). In order to improve the computational efficiency and stability of the model, a semi-implicit scheme is employed to produce a discrete form of the control equations (Casulli and Chen 1992). The water pressure gradient and bottom friction items are solved implicitly and the remaining terms are treated explicitly. With varying cell sizes, the curvilinear grid is flexible in generating fine grid cells at the coast and coarse ones at the open ocean. The CEST model uses a mass-balanced algorithm based on accumulated water volume to simulate the wetting-drying process and includes the land cover effect into the overland flooding. Bathymetric and topographic data are required for calculating the water depths and elevations of the grid cells in a model basin (Fig. 1). Further detail of model inputs, parameters and runs are provided in Table 2.

Goal 2 - Fate and Flux of Nutrients and Carbon: *Storm Deposits* - We used a spatially explicit sampling design (transects and discrete sampling points) during January 2018 to document storm deposit gradients associated with Hurricane Irma across mangrove sites in the Florida Coastal Everglades (FCE). Sites were selected along major river basins (upstream to downstream gradient) in southwestern Everglades including Shark River (SRS-5, 6, 7), Harney River (WSC-8, 9, 10), and Broad River (WSC-11, 12, 13) and Buttonwood Ridge, 1 km east from the mouth of Taylor River (Fig. 2). We measured the thickness, distribution, and physico-chemical properties of storm sediments using duplicate cores

collected along transects and discrete sampling points in FCE mangrove sites. All soil-sediment cores were collected with a piston core (2.5 cm diameter x 15 cm length) and sectioned into two layers, storm sediments (variable depths) and surface (top 10 cm) mangrove soils, and the depth of each layer was registered. The storm layer was easily distinguished from the mangrove layer due to its gray color, fine sandy texture, and organic-free content. All soil-sediment samples were oven-dried at 60ºC to a constant weight and weighted to determine bulk density (grams of dried mass per cm^3 of wet soil), organic matter content (% ashed-free dry weight), total nitrogen (N), and phosphorus (P) concentrations using standard protocols.

Forest Structure - Hurricane Irma's effects on mangrove forest structure were assessed from downstream to upstream locations along Shark River (SRS-5, 6, and 7 at 9, 4, and 0 km from the mouth, respectively) and Harney River (WSC-8, 9 and 10 at 10, 6 and 2 km from the mouth, respectively). At each site, vegetation plots (10 x 10 m) were established at 50, 100, and 350 m from the edge of the forest. All trees with diameter at breast height (DBH, 1.3 m) ≥ 5 cm were measured within each plot to determine species composition and tree density. We assessed the status of each tree including trunk condition (i.e., snapped, uprooted, inclined, no impact), tree live/dead, branch removal (%), and defoliation (%). Canopy openness was measured at each corner of the plots using a spherical crown densitometer (convex model A; Forestry Suppliers, Inc.); readings were collected at the four cardinal directions as replicates. The height of 10-15 live trees within plots was registered with a range finder (Forestry Pro, Nikon). We used the line-intercept technique originally proposed by Van Wagner (1968) and Brown (1974) and later applied to mangrove forests (Allen et al. 2000) to evaluate the spatial variation in woody debris (WD). At each plot, five 10 m transects were randomly established from the center of the plot and treated as replicates. Woody debris was measured at 1 m intervals along transects and coarse (≥7.5 cm in diameter) and fine (<7.5 cm in diameter) WD intersecting the line along the 10 m transect was measured to 0.1 cm with a DBH measurement tape. Standing aboveground (AG) wood biomass (live and dead) was calculated for each individual tree within plots using species-specific allometric equations published for the three-dominant mangrove species in the study area (Smith and Whelan 2006).

Biogeochemistry and Organic Matter Processing - We measured breakdown rates and root production (as ingrowth) rates in response to storm sediment deposits along the upstream-downstream coastal gradient of Shark River Slough (SRS). Salinity and soil phosphorus (P) concentrations increase from upstream to downstream along SRS (Chen and Twilley 1999; Castañeda-Moya et al. 2013; Breithaupt et al. 2018), but differences in root breakdown rates haven't been linked to differences in ambient soil P along SRS (Poret et al. 2007). We incubated triplicate root samples in two soil depths from 0 – 20 cm and 20 – 40 cm beginning 30 January 2018 for 190 d. There will be two more sampling events at 12 and 18 months. We collected a 40-cm soil core from each plot (n = 8 cores) using a 10-cm diameter PVC pipe. In the laboratory, we rinsed soils and collected only live roots identified by color and texture. Roots were subsequently air-dried and divided into three size classes of 1 – 4, 4 – 8, and 8 – 12 mm diameters. We filled 1-mm mesh bags (width: 10 cm, length: 40 cm) divided into two 20-cm sections with an equal mixture of each size classes (~5.8 g per depth). We incubated root decomposition bags buried at two sampling plots (n = 9 per plot) in each site (n = 18 per site). Triplicate root decomposition bags were harvested at all sites on 08 August 2018 for the first incubation interval. Collected samples were returned on ice. In the laboratory, samples were rinsed with deionized water, oven dried at 60°C for two weeks, and subsequently weighted for individual mass remaining. The decay constant, k, was calculated over sampling intervals with an exponential decay equation: $y = e^{-kt}$, where y is the fraction of initial mass remaining at time t.

Goal 3 - Consumer Responses via Trophic Pathways and Distributional Shifts: We are using acoustic telemetry to track the movement of large-bodied predators in the Shark River, adding to a continuous dataset extending back to 2007. Our seasonal sampling has focused on tagging Common Snook (*Centropomus undecimalis*), Largemouth Bass (*Microperus salmoides*), juvenile Bull Sharks (*Carcharhinus leucas*), and American Alligator (*Alligator mississippiensis*). Sampling efforts subsequent

to Hurricane Irma (post-9/10/2017) have resulted in the tagging of 19 additional Snook, 18 bass, 23 sharks, and 8 alligators (69 new tags deployed total). In addition, we have 29 Snook, 12 bass, 12 shark and 8 alligator tags deployed before Hurricane Irma that are still active. All movement records have been downloaded and compiled through June 2018, and we will update the dataset with the next acoustic receiver download in December, 2018.

Specific Objectives

Goal 1 - Model Verification and Impact Assessment:

1. Characterize the extent of storm surge deposits, elevation changes and forest structural damage along coastal estuaries.
2. Update and validate our storm surge attenuation model

Goal 2 - Fate and Flux of Nutrients and Carbon:

1. Evaluate sediment characteristics, distribution and thickness of sediments deposited by Hurricane Irma across FCE mangrove sites.
2. Assess the relative inputs of total N and P from hurricane deposits to the nutrient pools accumulated in mangrove soils.
3. Assess changes in canopy cover, aboveground biomass, and mortality rates in FCE mangroves as result of Hurricane Irma's impacts.
4. Determine the relative contribution of downed wood to the total (live + dead) standing biomass in mangroves of southwestern Everglades.
5. Quantify differences in mangrove root breakdown (*k*) along an upstream-downstream coastal gradient in FCE mangrove sites following Hurricane Irma.
6. Quantify differences in mangrove root production along an upstream-downstream coastal gradient in FCE mangrove sites following Hurricane Irma.
7. Relate differences in mangrove root *k* and production to P concentrations in sediment deposits and soil, and mangrove canopy damage associated with Hurricane Irma.

Goal 3 - Consumer Responses via Trophic Pathways and Distributional Shifts:

1. Use our acoustic telemetry array in the Shark River to examine the possibility of large-scale mortality and modifications of movement patterns of mobile consumers post-Irma.
2. Test whether distributional patterns and space use have shifted in response to changing abiotic and biotic conditions associated with the storm and post-storm recovery.

Significant Results

Goal 1 - Model Verification and Impact Assessment: The maximum peak storm tide height during Hurricane Irma was about 14 feet from CEST (Fig. 3). The time series of computed storm tides indicates that CEST reproduced the patterns of measured storm tides well at almost all stations, except Station Cedar Key (Fig. 4). Vegetation damage assessments, sediment deposition and Everglades tide data are among the field measurements being used to test computed storm surge against impacts of Hurricane Irma on the coastal Everglades. The gradient of computed storm surge heights ranged from about 10-12ft at the mouth of Broad River to 8-10ft at the mouth of Shark River (Fig. 5). Sampling sites well captured the range of variability in computed storm surge heights. Using USGS water level data, preliminary comparisons of phase and amplitude of the computed storm tides are comparable with the measured ones (Figs. 6, 7, 8). Computed and measured surge heights approximated 1.6-2ft, 3-5ft and 1.5-3ft for Broad, Harney and Shark River stations. Note the USGS station locations along each of the rivers do not coincide with locations where maximum storm surge was observed with computed CEST output.

Goal 2 - Fate and Flux of Nutrients and Carbon: *Storm Deposits* - Hurricane Irma created a large-scale mineral sediment deposition associated with the storm surge across FCE mangroves. Sediment deposition showed a distinct pattern with distance inland from edge at each of the mangrove transects (Fig. 9), and followed a similar trend as previously reported in the study area after the passage of Hurricane Wilma on October 24, 2005 (Castañeda-Moya et al. 2010). Maximum deposition was observed in mangrove sites closer to the mouth of estuaries compared to middle and upstream regions. accretion resulting from Hurricane Irma was up to 20 times greater than the annual accretion rate (0.27 ± 0.04 cm yr^{-1}; Breithaupt et al. 2014) averaged over the last 100 years across mangrove sites. Organic matter content was significantly lower in storm sediments (17.4 ± 1.5 mg cm^{-3}) compared to surface soils (42.5 ± 6.5 mg cm^{-3}) across transect sites, and consistently decreased with distance inland from the mouth of the estuaries, following the observed pattern previously reported along basins in southwestern FCE (Chen and Twilley 1999; Castañeda-Moya et al. 2013; Breithaupt et al. 2018; Fig. 10). Total N concentrations ranged from 1.7 ± 0.1 (WSC-13) to 2.5 ± 0.3 mg cm^{-3} (SRS-5) in storm deposits relative to 2.1 ± 0.1 (SRS-6) to 2.5 ± 0.1 mg cm^{-3} (Ridge) in surface soils (Fig. 11). Total P was on averaged 1.5 times higher in storm sediments (0.29 ± 0.04 mg cm^{-3}) compared to surface soils (0.19 ± 0.02 mg cm^{-3}), and consistently decreased with distance inland from the mouth of all estuaries, following same trend as previous studies (Chen and Twilley 1999; Castañeda-Moya et al. 2013; Breithaupt et al. 2018).

Forest Structure - Tree defoliation ranged from 39% (SRS-5) to 84% (SRS-7) across sites, with higher defoliation in downstream sites of Shark River and WSC-10 (Harney River; Fig. 12). Canopy openness followed a similar trend compared to tree defoliation and ranged from 28 to 71%. Along Shark River, canopy openness decreased from downstream to upstream regions likely due to differential hurricane wind fields intensity (Fig. 12). Similarly, there were differences in standing AG biomass between live and dead trees at all sites (Fig. 13). Higher dead biomass was observed in downstream sites of Shark River, WSC-8 and WSC-10. Notably, dead biomass accounted for 15% (SRS-5) to 52% (SRS-7) of the total biomass across all sites, with some sites showing a reduction in standing live biomass nearly by half (Fig. 13). Coarse WD accounted for 70-84% of the total downed wood across sites (Fig. 14). Tree mortality was variable across sites, with higher rates in downstream sites of Shark (SRS-7) and Harney (WSC-10) Rivers (Fig. 15). Remarkably, the upstream site WSC-8 (Harney) showed high mortality and defoliation rates, but the lowest estimates of downed wood. Overall, higher mortality rates (50-73%) of bigger trees (DBH >10 cm) were observed in downstream sites at both basins. In contrast, smaller trees (DBH <10 cm) accounted for most (50%) of mortality in upstream sites of Shark (SRS-5) and Harney (WSC-8) Rivers (Fig. 15).

Biogeochemistry and Organic Matter Processing – Our long-term biogeochemistry data clearly show the influence of Hurricane Irma on constituent fluxes in Shark River Slough, with spikes in both total phosphorus and dissolved organic carbon occurring immediately following the storm (Figs. 16, 16). Root decomposition rates ranged from 0.007 (median at SRS-6) to 0.012 d^{-1} (median at SRS-7; Fig. 18). Averaging across both soil depths, breakdown rates were lowest at SRS-6 (0.007 ± 0.001 d^{-1}, mean ± standard deviation) and highest at SRS-7 as of (0.012 ± 0.001 d^{-1}) that were significantly different (Tukey HSD, $P < 0.001$). Depth-specific differences in root k at SRS-5 showed that k was higher at 0 – 20 cm than 20 – 40 cm (Tukey HSD, $P < 0.01$). Higher root breakdown rates were previously measured at SRS-5 than SRS-4 and SRS-6, which were attributed to lower initial N concentrations and lignin content in mangrove roots from SRS-5 (Poret et al. 2007).

Goal 3 - Consumer Responses via Trophic Pathways and Distributional Shifts: To investigate how disturbances resulting from Hurricane Irma (landfall 9/10/2017) correlated with animal movement, we compiled data on rapidly changing environmental conditions surrounding the storm (Fig. 19). Analysis of our telemetry data revealed large-scale movements of Common Snook (*Centropomus undecimalis*) in the time period surrounding hurricane landfall (Fig. 20). All 22 fish detected were initially located in the upper river, and 73% (16 Snook) moved downstream into different habitat zones, deviating from pre-

storm behavior and typical movements patterns associated with local foraging behaviors. A total of 75% of these moving fish (12 Snook) relocated to Tarpon Bay, and 25% (4 Snook) moved rapidly downstream and were last detected on receivers near the coast, suggesting a potential exit from the system. A multi-model selection process using logistic regression analysis indicated that these movements were best explained by a combination of low barometric pressures and rising water levels in the upper river. In the six months following the hurricane, 25% of the fish returned to the upper river, 6% remained in Tarpon Bay, 19% were detected moving among river zones, 19% were redetected on coastal receivers, and 31% were not re-detected, suggesting either mortality or an exit from the system. We also detected effects of Hurricane Irma on the movements patterns of juvenile Bull Sharks (*Carcharhinus leucas*). All 14 sharks detected during Irma appeared to attempt to leave the shallow waters of the estuary before the hurricane impact, but individuals varied in the timing and success of these movements (Fig. 21). A total of 3 sharks (~21%) moved downstream relatively late and appear to have died before leaving the system. Of the sharks last detected on the most downstream monitors, indicative of exiting the estuary, 9 of 11 sharks (~82%) eventually returned to the array within weeks or months of the storm. Several individuals (6 of 11, ~55%) were detected on monitoring stations in coastal waters *ca.* 80 km away from the mouth of the SR Estuary. We also monitored the responses of 8 alligators to Hurricane Irma. Four animals (50%) exhibited no difference in movement patterns or their use of macro-habitats within the estuary before, after, or during the storm. Three animals (~38%) retreated to more inland marsh habitats (outside receiver detection ranges) and remained absent from the array. Interestingly, one animal (~13%) took multiple excursions to the coast immediately before and for months after the hurricane. This animal had not visited the river mouth in the year prior.

Key Outcomes or Other Achievements

Our results highlight the distinct pattern of sediment deposition and nutrient inputs across mangrove sites, from the edge to the interior of the forest, and with distance inland from the mouth of estuaries. Allochthonous mineral inputs from Hurricane Irma represent a significant source of sediment to vertical accretion and nutrient resources in mangroves of southwestern Everglades. This sediment and nutrient input may serve as a natural fertilization mechanism that contributes to soil P fertility and to the rapid recovery of mangroves as has been documented after the passage of Hurricane Wilma across the FCE in October 2005. This positive feedback from hurricane P deposition is particularly significant to mangrove forest development due to the P-limited condition of this carbonate ecosystem. This source of P may be an important adaptation of mangroves in regions with high recurrence of hurricanes such as the Gulf of Mexico and Caribbean regions to projected impacts of sea-level rise.

Our results underscore the differential physical damage of mangrove vegetation in response to hurricane disturbance. This is particularly significant given that the effects of Irma were not the same along sites in both basins, with higher damage in mangrove areas closer to the mouth of estuaries. Moreover, in contrast to Shark River, some upstream areas (WSC-8; 10 km from the mouth) in Harney River were also heavily affected, with significant defoliation and tree mortality, but low input of downed wood. This spatial variability in tree damage along estuaries reflects differential hurricane intensity, direction, and wind fields action as the storm approached and made landfall in the southwestern Florida coast, creating gradients of impact, with higher overall effects in mangrove areas closer to the mouth of estuaries. These findings are significant to our understanding of the resilience (i.e., magnitude and rate) capacity of FCE mangroves to the disturbance regime. Current structural and functional mangrove attributes reflect a range of return to pre-disturbance levels following the passage of Hurricane Wilma (Danielson et al. 2017). Therefore, trajectories of mangrove recovery after Irma's impact will be a function of disturbance parameters (e.g., intensity, duration, and trajectory) that interact with legacies of previous storms, and the intrinsic long-term ability of mangrove species to cope with disturbance effects. Our long-term research provides a robust framework to continue assessing resilience and the role of hurricane disturbances on the structure and function of south Florida mangroves.

Predicting the responses of animals to environmental changes is a fundamental goal of ecology and is necessary for conservation and management of species. While most studies focus on gradual changes, extreme events may have profound and lasting impacts on populations. Animals may respond to major disturbances such as hurricanes by seeking shelter or migrating or they may fail to appropriately respond. Our results suggest that sharks took advantage of multiple cues including declining barometric pressure and fluctuations in river stage and discharge to decide when to leave the estuary. Extreme events may be an adequate selective pressure to result in behaviors tied to appropriate and non-fatal responses. Movement can carry widespread and diverse implications, and by better understanding the factors that drive movement, we may anticipate how future extreme climate events could affect animal populations in the Everglades. Sister manuscripts detailing the results of these analyses were submitted to Estuaries and Coasts in September, 2018, for publication in a special issue on the 2017 hurricane season.

We have submitted a cross-site coastal ecosystems workshop proposal (*Ecosystem Responses to Hurricanes Synthesis Workshop*) to NSF DEB Ecosystems Panel to to understand how ecosystems respond to hurricanes so that we may make predictions about coastal ecosystems under future climate scenarios and develop corresponding management strategies to increase coastal resilience. Chris Patrick (PI, Texas A&M Corpus Christi), John Kominoski (Co-PI, Florida International University & Florida Coastal Everglades LTER), and William McDowell (Co-PI, University of New Hampshire & Luquillo LTER) propose involving partners from non-LTER coastal sites as well as collaborators at the Georgia Coastal Ecosystems (GCE) and Luquillo (LUQ) LTER sites to compare and synthesize findings from recent hurricanes. Specifically, we will compare ecosystem resilience to different types of tropical storm impacts, from wind and storm surge in subtropical marshes (FCE and Gulf of Mexico), to storm surge impacts on coastal temperate saltmarshes (GCE), to wind and torrential rain impacts on tropical montane rainforests (LUQ). Collectively, proposed research from these three LTER sites will fill large knowledge gaps in our understanding of disturbance impacts and interactions among legacies across a broad range of ecosystem types.

We initiated a research collaboration with Dr. David Lagomasino (NASA Goddard Space Flight Center & University of Maryland) and Dr. Lola Fatoyinbo (NASA Goddard Space Flight Center) to assess landscape changes in mangrove canopy volume (foliage, branches, stems), aboveground biomass, and mortality as a result of Hurricane Irma's effects on FCE mangroves. NASA has conducted airborne campaigns using LiDAR Hyperspectral & Thermal Imager (G-LiHT) tools before (May 2017) and after (November 2017) the passage of Irma across south Florida to assess storm damage on mangrove forests. In addition, during the field campaign in January 2018, NASA researchers conducted ground scans (1 m intervals) using a compass biomass lidar and terrestrial recording of 3D 360 surveys along transects. Remote sensing, hyperspectral and field data coupled with our forest structure surveys will allow us to develop site-specific digital terrain models (1 m resolution) of mangrove structural attributes and to estimate landscape changes in mangrove vegetation cover and biomass and as result of hurricane disturbance in the Florida Everglades.

Opportunities for training and professional development

Our project has been able to train six undergraduate (two female, four underrepresented minority), two research technicians (Diana Johnson, Amanda Kuhn), two graduate students (Meredith Emery and Lukas Lamb-Wotton), and a minority postdoc (Dong Yoon Lee) from the Department of Biological Sciences at Florida International University. Researchers participated during field data collection and were involved in the analysis of soil and root material samples collected during the mangrove field campaigns in January and July 2018. Students participated during field data collection and were involved in the analysis of soil and plant material samples collected during the mangrove field campaign in January 2018.

How have the results been disseminated to communities of interest?

Presentations:

Castaneda, E., D. Lagomasino, T. Troxler, and E. Gaiser. Effects of Hurricane Irma on mangrove forest structure in the Florida Coastal Everglades (FCE). LTER Network All Scientists' meeting. September 30th to October 3rd, 2018. Pacific Grove, CA.

Gaiser, E.E. Hurricanes as resilience builders. National Science Foundation & Long Term Ecological Research Symposium, National Science Foundation, Washington, D.C. April 16, 2018.

Gaiser, E. 2018. Surface tensions: Harnessing the connecting power of water for a sustainable future. Association for the Science of Limnology and Oceanography. Closing Plenary Presentation, Victoria, BC.

Kominoski, J.S., E. Castañeda-Moya E.E. Gaiser, D.Y. Lee et al. Quantifying biogeochemical changes in coastal ecosystems exposed to vegetation shifts and saltwater intrusion. Invited Seminar. Department of Marine Sciences, University of Georgia, Athens, GA. October 29, 2018.

Lass, P., K. Ugarelli, R. Travieso, S. Stumpf, H. Briceno, E. Gaiser, J. Kominoski, U. Stingl. Microbial communities in waters of the Florida Coastal Everglades were impacted by Hurricane Irma. Poster. LTER Network All Scientists' meeting. September 30th to October 3rd, 2018. Pacific Grove, CA.

Massie, J.A., R. Santos, B. Stricland, J. Hernandez, N. Viadero, H. Willoughby, M. Heithaus, and J. Rehage. Environmental drivers of large-scale fish movements in the Florida Everglades during Hurricane Irma. Poster. LTER Network All Scientists' meeting. September 30th to October 3rd, 2018. Pacific Grove, CA.

Rugge, M., Gaiser, E., J. Kominoski, J. Rehage, K. Grove, J. Fourqurean. 2018. Drivers of abrupt change in the Florida Coastal Everglades. Poster. LTER Network All Scientists' meeting. September 30th to October 3rd, 2018. Pacific Grove, CA.

Publications:

Davis, S.E., R. Boucek, E. Castaneda-Moya, S. Dessu, E. Gaiser, J. Kominoski, J.P. Sah, D. Surratt, and T. Troxler. 2018. Episodic drivers affecting water quality in the Florida Coastal Everglades: A Ridge to Reef Perspective. *Ecosphere*. (6):e02296. 10.1002/ecs2.2296

Workshops:

Lagomasino, D., E. Castañeda-Moya, E. Gaiser, and J. Kominoski. 2018. Synthesizing long-term research field and remote sensing data on major ecological disturbances. LTER Network All Scientists' meeting. September 30th to October 3rd, 2018. Pacific Grove, CA.

Grimm, N., A. Lugo, C. Boone, D. Iwaniec, J. Kominoski, M. Blasquez, M. Smith, M. Grove, and S. Pickett. Understanding and responding to extreme events in ecosystems and social-ecological-technical systems. LTER Network All Scientists' meeting. September 30th to October 3rd, 2018. Pacific Grove, CA.

Gaiser, E., D. Childers, J. Kominoski, J. Ripplinger, P. Groffman, and S. Pickett. Contributions of long term ecological research to changing theoretical paradigms of disturbance ecology. LTER Network All Scientists' meeting. September 30th to October 3rd, 2018. Pacific Grove, CA.

Gaiser, E., D. Childers, J. Kominoski, J. Ripplinger, P. Groffman, and S. Pickett. Contributions of long term ecological research to changing theoretical paradigms of disturbance ecology. LTER Network Webinar, July 2018.

Gaiser, E., E. Castaneda, J. Kominoski, J. Rehage, J. Zimmerman, S. Pennings, and J. E. Lopez. Updates on the impacts of the 2017 hurricane season on subtropical ecosystems. Florida Coastal Everglades Long Term Ecological Research program All Scientists Meeting. Miami, FL. May, 2018.

Media:

Interview with Dr. Evelyn Gaiser: “The Everglades have always been hit by hurricanes. Thanks to climate change, Irma could be a different matter.” *The Washington Post*
http://wapo.st/2y1SppX?tid=ss_mail&utm_term=.48366b505a4e

Interview and photos from Dr. Steve Davis: “After Irma, dead seagrass 'as far as the eye can see' in Florida Bay.” *Miami Herald*
http://www.miamiherald.com/news/weather/hurricane/article173637481.html

Interview with Dr. Danielle Ogurcak: “How Hurricane Irma Could Affect Florida's Endangered Species.” *Science Friday*
https://www.sciencefriday.com/person/danielle-ogurcak/

Interview with Dr. Fernando Miralles-Wilhelm: “The Everglades After Irma” *Living on Earth*
http://www.loe.org/shows/segments.html?programID=17-P13-00037&segmentID=2

Interview with Dr. Edward Castaneda-Moya: “” *BBC Our Blue Planet*
https://www.facebook.com/bbcearth/videos/301586387104444/
https://twitter.com/BBCEarth/status/1048257760612245504

What do you plan to do next year?

In the coming year of our no-cost extension, we plan to: (1) complete validation of our storm surge attenuation model, (2) analyze the results of this study in the context of our long-term datasets, (3) hold a workshop with collaborators from other locations to synthesize results, (4) publish a special issue in the journal Estuaries and Coasts focused on the effects of the 2017 hurricane season (editors: Wachnicka and Fourqurean), (5) continue network-scale disturbance syntheses resulting in two manuscripts, (6) complete at least four additional manuscripts summarizing the effects of Hurricane Irma. Specific steps in our modeling synthesis to complete include: 1) compute and analyze measured and computed data, including other USGS stations, 2) evaluate the extent of sediment deposition and how it correlates with computed storm surge heights, 3) consider the impacts of wind vs. water in vegetation damage assessments and 4) consider ways in which Manning’s n can be improved with quantitative measurements of vegetation structure and damage (i.e. projected area, vertical integration of forest stand morphological structure).

References

Allen, J.A., K.C. Ewel, B.D. Keeland, T. Tara, and T.J. Smith, III. 2000. Downed wood in Micronesia mangrove forests. *Wetlands 20: 169-176*.

Blumberg, A., & Kantha, L. (1983). Open boundary condition for circulation models. *Journal of Hydraulic Engineering, 112*, 237-255

Breithaupt, J.L. J.M. Smoak, C.J. Sanders, and T.G. Troxler. 2018. Spatial variability of organic carbon, $CaCO_3$ and nutrient burial rates spanning a mangrove productivity gradient in the coastal Everglades. *Ecosystems. doi.org/10.1007/s10021-081-0306-5*.

Breithaupt, J.L. J.M. Smoak, T.J. Smith, III., and C.J. Sanders. 2014. Temporal variability of carbon and nutrient burial, sediment accretion, and mass accumulation over the past century in a carbonate platform mangrove forest of the Florida Everglades. *Journal of Geophysical Research: Biogeosciences 119: 2032-2048. doi:10.1002/2014JG002715.*

Brown, J.K. 1974. Handbook for inventorying downed woody material. USDA. Forest Service, Intermountain Forest and Range Experiment Station, Ogden, Utah, USA. General Technical Report INT-16.

Castañeda-Moya, E., R.R. Twilley, and V.H. Rivera-Monroy. 2013. Allocation of biomass and net primary productivity of mangrove forests along environmental gradients in the Florida Coastal Everglades, USA. *Forest Ecology and Management 307: 226-241.*

Castañeda-Moya, E., R.R. Twilley, V.H. Rivera-Monroy, K. Zhang, S.E. Davis III, and M. Ross. 2010. Sediment and nutrient deposition associated with Hurricane Wilma in mangroves of the Florida Coastal Everglades. *Estuaries and Coasts 33: 45-58.*

Casulli, V., & Chen, R.T. (1992). Semi-implicit finite difference method for three-dimensional shallow water flow. *International Journal for Numerical Methods in Fluids, 15*, 629-648

Chen, R., and R.R. Twilley. 1999. Patterns of mangrove forest structure and soil nutrient dynamics along the Shark River Estuary, Florida. *Estuaries 22: 955-970.*

Danielson, T.M., V.H. Rivera-Monroy, E. Castaneda-Moya, H. Briceno, R. Travieso, B.D. Marx, E. Gaiser, and L.M. Farfan. 2017. Assessment of Everglades mangrove forest resilience: Implications for above-ground net primary productivity and carbon dynamics. *Forest Ecology and Management 404: 115-125*.

Fry, J., Xian, G., Jin, S., Dewitz, J., Homer, C., Yang, L., Barnes, C., Herold, N., & Wickham, J. (2011). Completion of the 2006 National Land Cover Database for the Conterminous United States. *Photogrammetric Engineering and Remote Sensing, 77*, 858-864

LeMehaute, B. (1976). *An introduction to hydrodynamics and water waves*. New York, USA: Springer-Verlag

Poret, N., R.R. Twilley, V.H. Rivera-Monroy, C. Coronado-Molina. Belowground decomposition of mangrove roots in the Florida Coastal Everglades. 2007. *Estuaries and Coasts 30: 491-496. https://doi.org/10.1007/BF02819395*

Jelesnianski, C.P., Chen, J., & Shaffer, W.A. (1992). SLOSH: Sea, lake and overland surges from hurricanes. In (p. 71). Washington, D.C.: NOAA

Mattocks, C., & Forbes, C. (2008). A real-time, event-triggered storm surge forecasting system for the state of North Carolina. *Ocean Modelling, 25*, 95-119

Mukai, A.Y., Westerink, J.J., Luettich, R.A., & Mark, D. (2002). Eastcoast 2001, A Tidal Constituent Database for Western North Atlantic, Gulf of Mexico, and Caribbean Sea. In (p. 23). Vicksburg, Mississippi: U.S. Army Corps of Engineers

Van Wagner, C.E. 1968. The line intersect method in forest fuel sampling. *Forest Science 14: 20-26.*

Zhang, K., Liu, H., Li, Y., Xu, H., Shen, J., Rhome, J., & Smith III, T.J. (2012). The role of mangroves in attenuating storm surges. *Estuarine, Coastal, and Shelf Science, 102-103*, 11-23

Zhang, K., Li, Y., Lui, H., Rhome, J., & Forbes, C. (2013). Transition of the Coastal and Estuarine Storm Tide Model to an operational forecast model: A case study of Florida. *Weather and Forecasting, DOI:10.1175/WAF-D-12-00076.1*

Tables and Figures

Table 1. South Florida Basin description and model detail.

Basin Name	**SF**
Domain Description	South Florida Basin
Resolution (m)*	175
Dimension	425*1500
Total Number of Cells	637,500
Time Step (s)	30
Computation Time* of 4 days (hours)	6-8

*The resolution of the model basin varies spatially. The resolution in the table represents the approximate edge size of a grid cell at the coastal area. Computation time was derived by recording the simulation time using a single processor in a Dell PC workstation with four 2.5 GHZ Intel Xeon processors and 16GB of RAM.

Table 2. Model components

1. Topographic and bathymetric Data and Calculation of Grid Cell Elevation	The topographic data used in this study mainly come from the US Geological Survey (USGS) and South Florida Water Management District (SFWMD), and the bathymetric data come from NOAA. The SFWMD 5-m digital elevation model (DEM) data was used to derive the elevation over the fine-resolution model grid if the data were available for the study area (http://apps.sfwmd.gov/gisapps/sfwmdxwebdc/). The Florida Geographic Data Library (FGDL) 5-m DEM data were used for areas without SFWMD DEMs (https://www.fgdl.org/metadataexplorer/explorer.jsp). The USGS 90 m, 30 m, or 10 m digital elevation models (DEM) were used to calculate the elevation of grid cells on the land (http://viewer.nationalmap.gov/viewer/) if SFWMD and FGDL data are not available. NOAA 2-minute Global Relief Model (ETOPO2) and 3-arc-second Coastal Relief Model were combined to obtain bathymetric data for the model grid. Water depths for grid cells in coastal areas were interpolated from the U.S. coastal relief dataset from NOAA with a resolution of 3 arc second (~90 m) (http://www.ngdc.noaa.gov/mgg/gdas/gd_designagrid.html).
2. Calculation of Manning's Coefficients Using Land Cover Data	The CEST model uses the Chezy formula (LeMehaute 1976) with a Manning's roughness coefficient to calculate bottom stresses. Manning's coefficients for grid cells over the land were estimated according to the 2006 national land cover dataset (NLCD) created by the U.S. Geological Survey (USGS) (Fry et al. 2011). A modified table of Manning's coefficients corresponding to different land cover categories (Mattocks and Forbes, 2008; Zhang et al., 2012) was employed in this study. Since the spatial resolution of NLCD is 30 m which is usually smaller than the cell size of a CEST grid, an average Manning's coefficient (na) for a grid cell was calculated using $n_a = \frac{\sum_{i=1}^{N}(n_i\alpha) + n_w\beta}{N\alpha + \beta}$ where ni is the Manning's coefficient value of a NLCD pixel within a model grid cell, α is the area of a NLCD pixel, N is the total number of NLCD pixels within a model cell, nw is the Manning's coefficient for the oceanic area β that are not covered by NLCD pixels.
3. Open Boundary Conditions	The "Sommerfield" radiation condition (Blumberg and Kantha 1983) was used at the open boundaries for a variable □ which can be either water level or velocity: $\frac{\partial\phi}{\partial t} + \hat{c}\frac{\partial\phi}{\partial n} = 0$ where $\hat{c}$ is the velocity which includes wave propagation and advection. The water level elevation at the open boundary was generated using seven tidal constituents M2, S2, N2, K1, O1, K2, and Q1. These constituents were obtained from the U.S. Army Corps of

	Engineers' USACE) East Coast 2001 database of tidal constituents (Mukai et al. 2002).
4. Wind field computation	The parametric wind model used by the Sea, Lake, and Overland Surge from Hurricane (SLOSH) model (Jelesnianski et al. 1992) was employed to estimate the hurricane wind field. To account for the terrain effect on the wind, two different drag coefficients are used to compute the wind field on the terrain and extreme shallow waters and the wind field on the ocean, which are referred to as lake wind and ocean wind, respectively. The effects of vegetation on the wind field have also been accounted for in a way similar to the SLOSH model. The wind speed is adjusted using a coefficient C_T based on the ratio of the surge water depth (D=H+ζ) to the vegetation height (H_T): $$C_T = \begin{Bmatrix} \frac{D}{H_T} & D < H_T \\ 1 & \mathrm{D} \geq \mathrm{H_T} \end{Bmatrix}$$ The effect of trees on the wind speed decreases based on this equation as the water submerges the vegetation gradually. In this study, the land areas covered by dense vegetation and development were classified into the "Tree" category and assigned an average vegetation height of 8 m, the same as the one used by SLOSH for the Florida basins. When a storm surge floods low-lying areas, it often forms a thin layer of water over land. An extinction coefficient C_E is applied to the wind speed to reduce its effect on the thin layer of water (Jelesnianski et al. 1992). $$C_E = \begin{Bmatrix} \frac{D}{0.3} & D < 0.3\ m \\ 1 & D \geq 0.3\ m \end{Bmatrix}$$
5. Simulation of Hurricane Irma	The CEST model solves the continuity and full momentum equations which are forced by winds, atmospheric pressure drops, and astronomical tides or a time series of water levels at open boundaries. Storm tide simulation for Hurricane Irma was conducted, starting at 0100 coordinated universal time (UTC) September 08 and ending at 0100 UTC September 12, 2017, continued for 4 days. The initial water level was set to be 0.3 m above the NAVD88 based on the analysis of tide gauge records in the basins prior to the passing of Irma.

Figure 1. The locations of NOAA tide gauges at South Florida also showing the elevations/water depths of the grid cells.

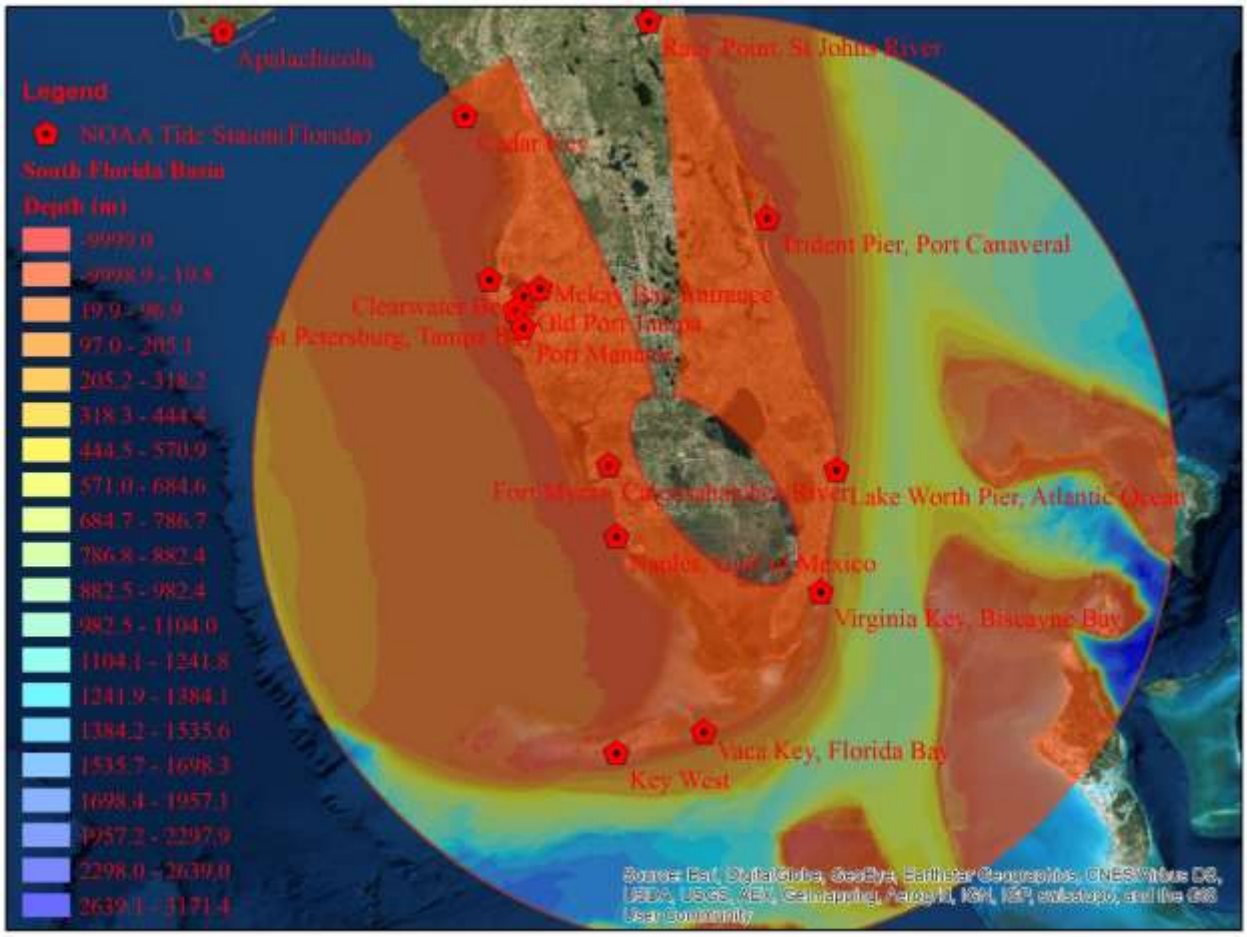

Figure 2. Location of the study sites in the Everglades National Park (ENP). SRS-4, 5, 6 along Shark River and TS/Ph-6, 7 are part of the Florida Coastal Everglades Long-term Ecological Research (FCE-LTER) program.

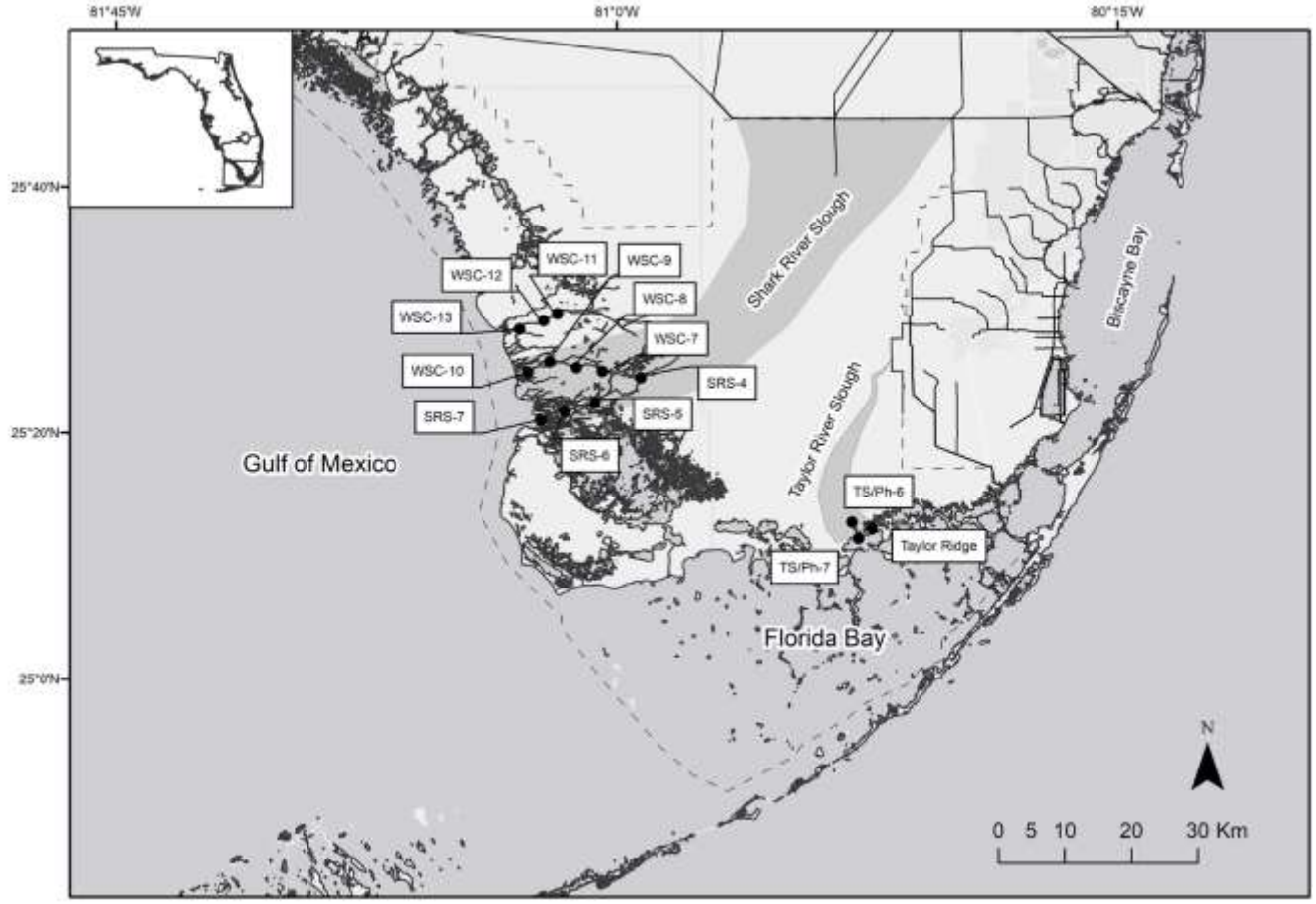

Figure 3. Computed peak storm tide heights caused by Hurricane Irma above the NAVD 88 computed from CEST. The maximum peak storm tide height is about 14 feet from CEST.

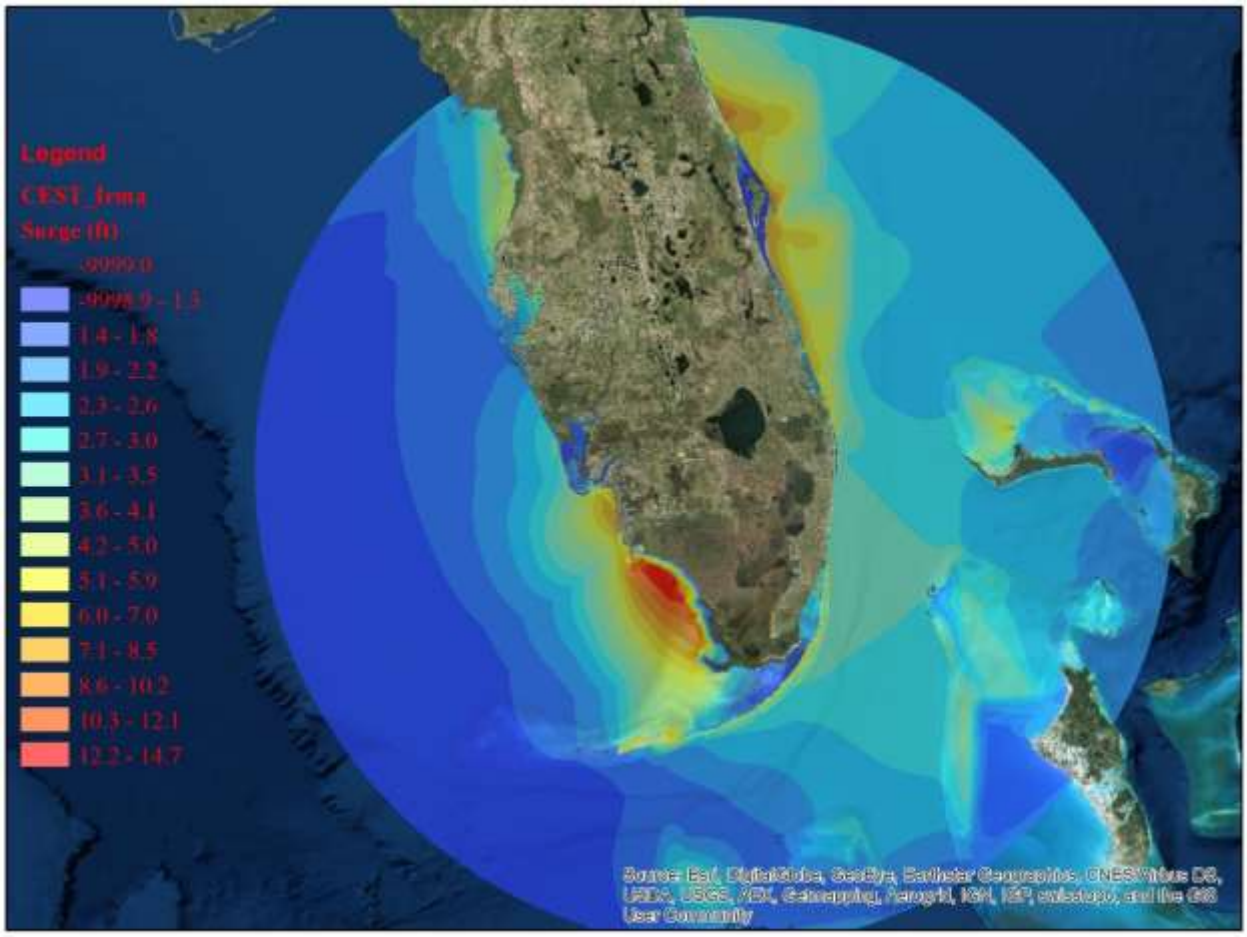

Figure 4. Computed storm surges (red line) vs. measured water levels (black line) at 9 NOAA tidal stations during Hurricane Irma.

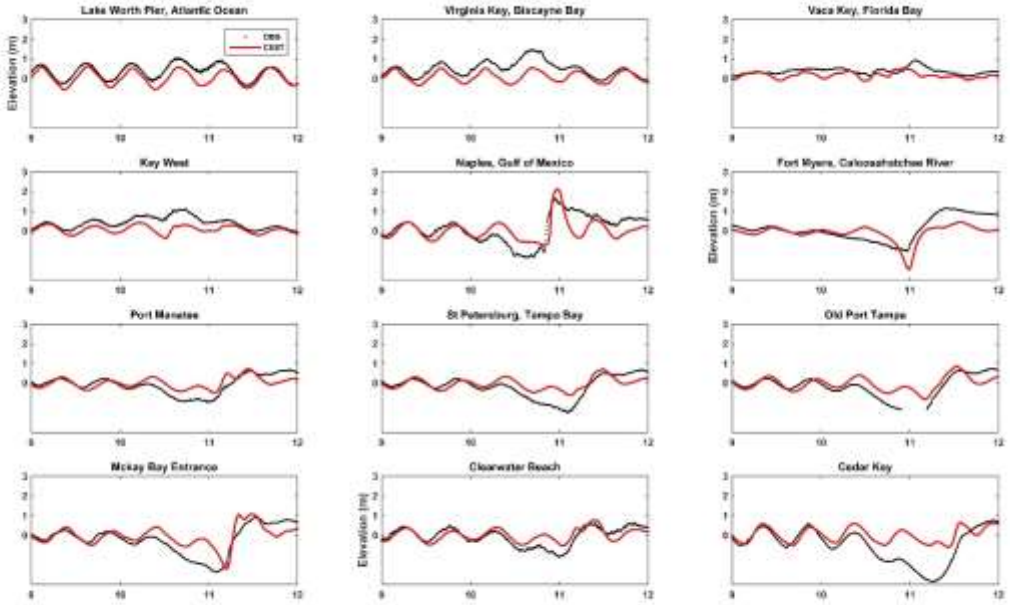

Figure 5. CEST-computed storm surge heights and vegetation sampling stations along Broad, Harney and Shark Rivers in the coastal Everglades.

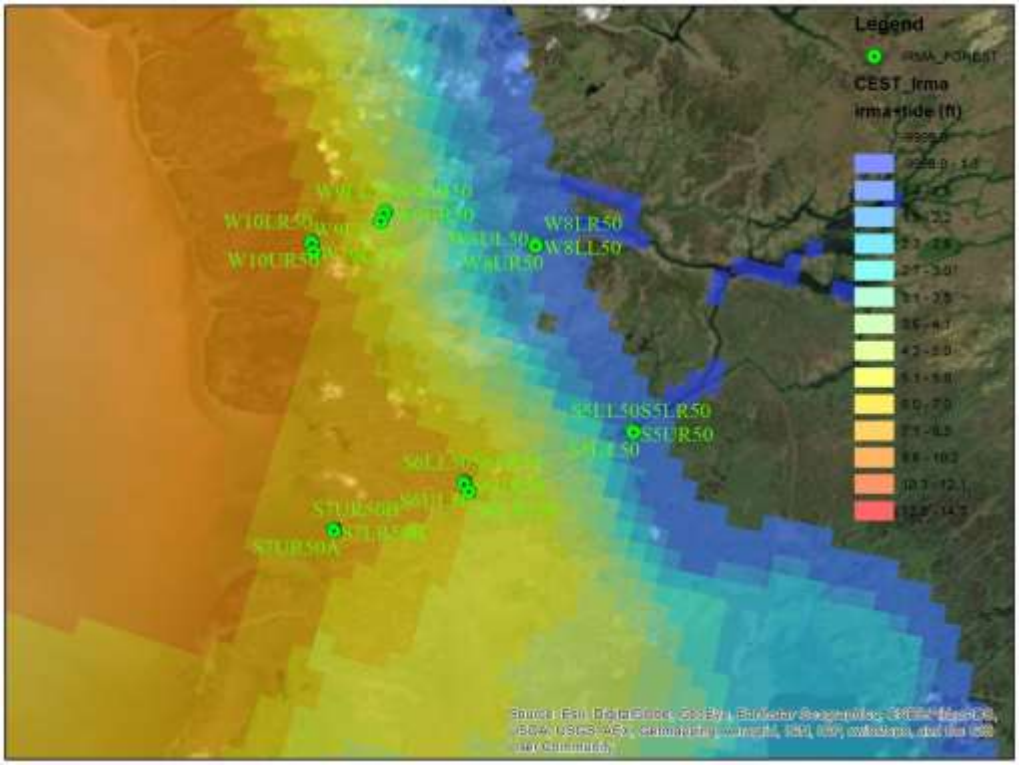

Figure 6. CEST-computed storm surge heights and vegetation sampling stations along Broad, Harney and Shark Rivers in the coastal Everglades.

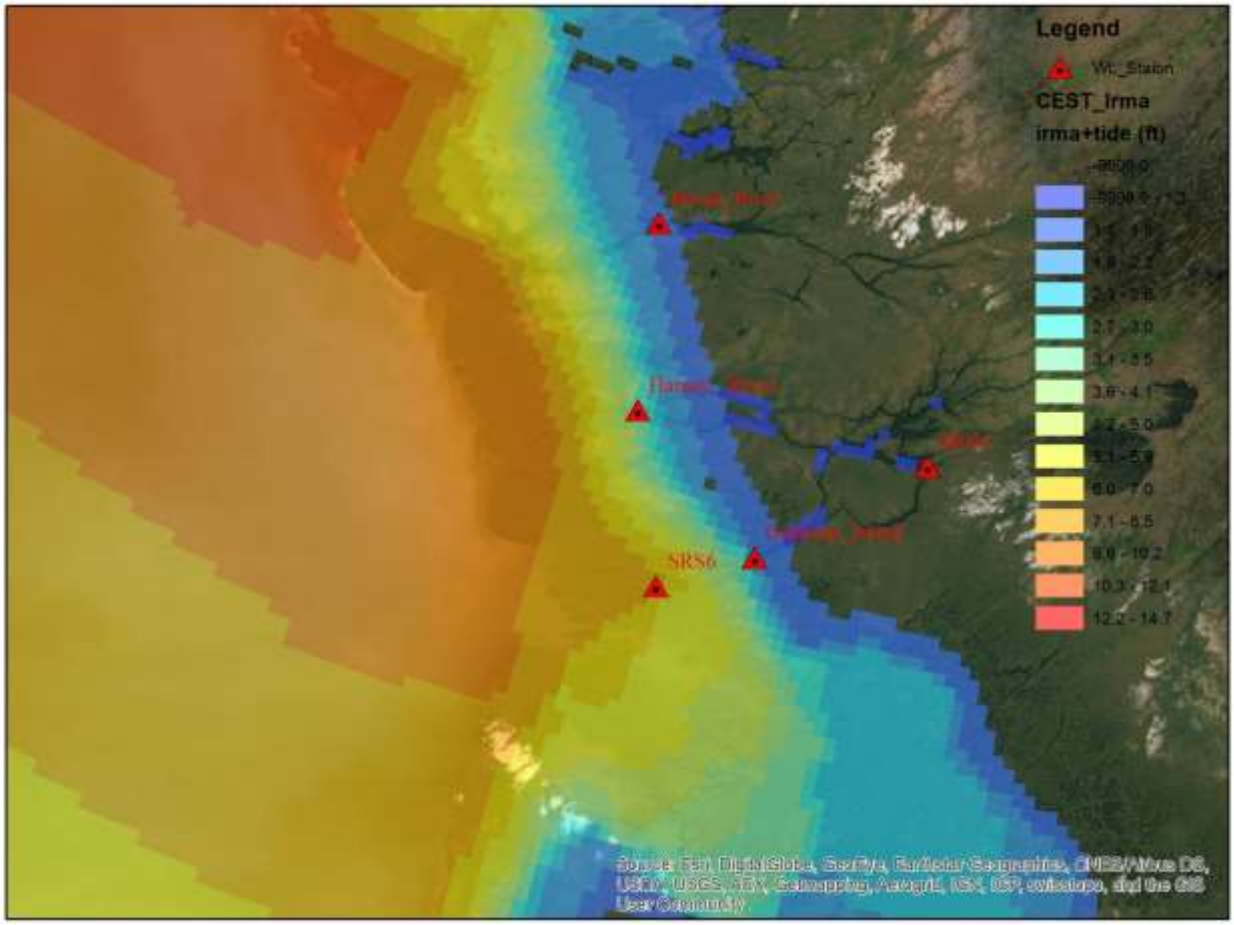

Figure 7. Measured water levels and surge heights (~ September 10, 2017) at USGS stations along Broad, Harney and Shark Rivers.

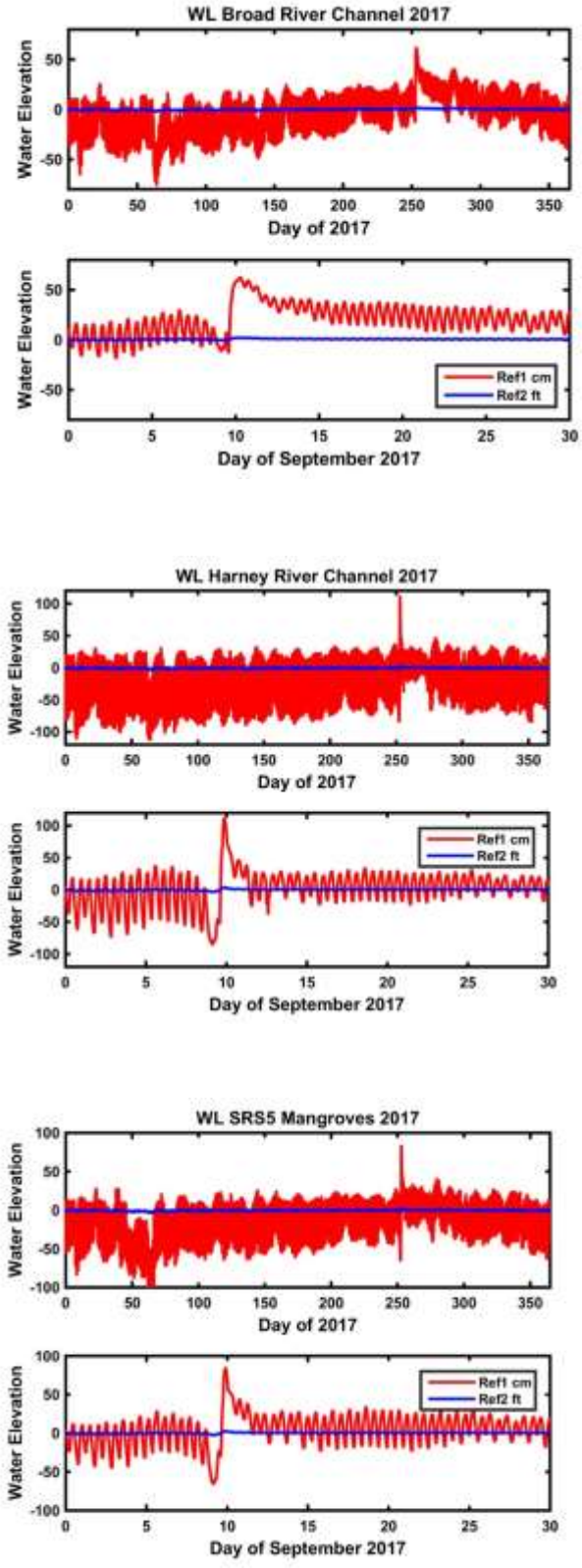

Figure 8. Continuous daily water depth data from FCE sites in Shark River Slough from 2011-2017 showing sustained increase in water depth during the period following Hurricane Irma (10 Sept 2017).

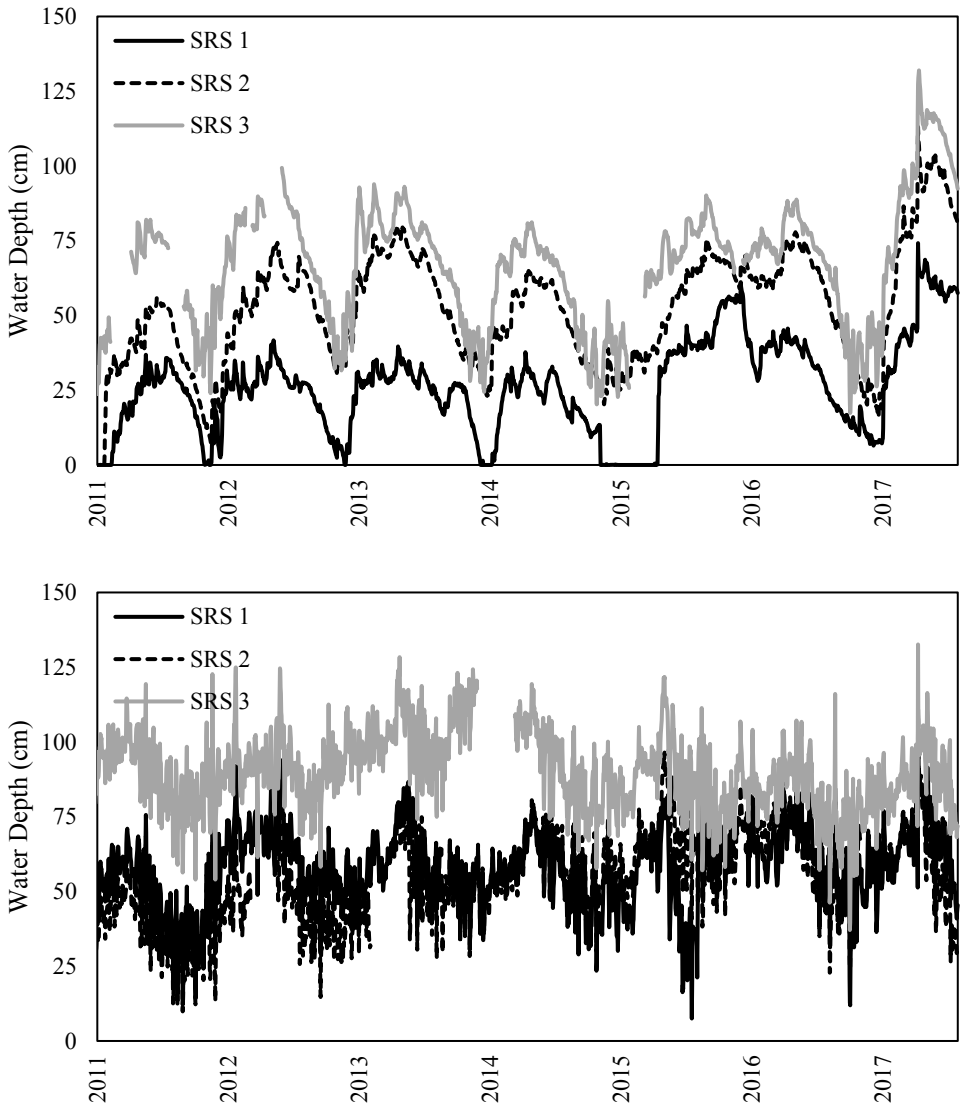

Figure 9. Depth of storm sediments at mangrove sites in the Florida Coastal Everglades.

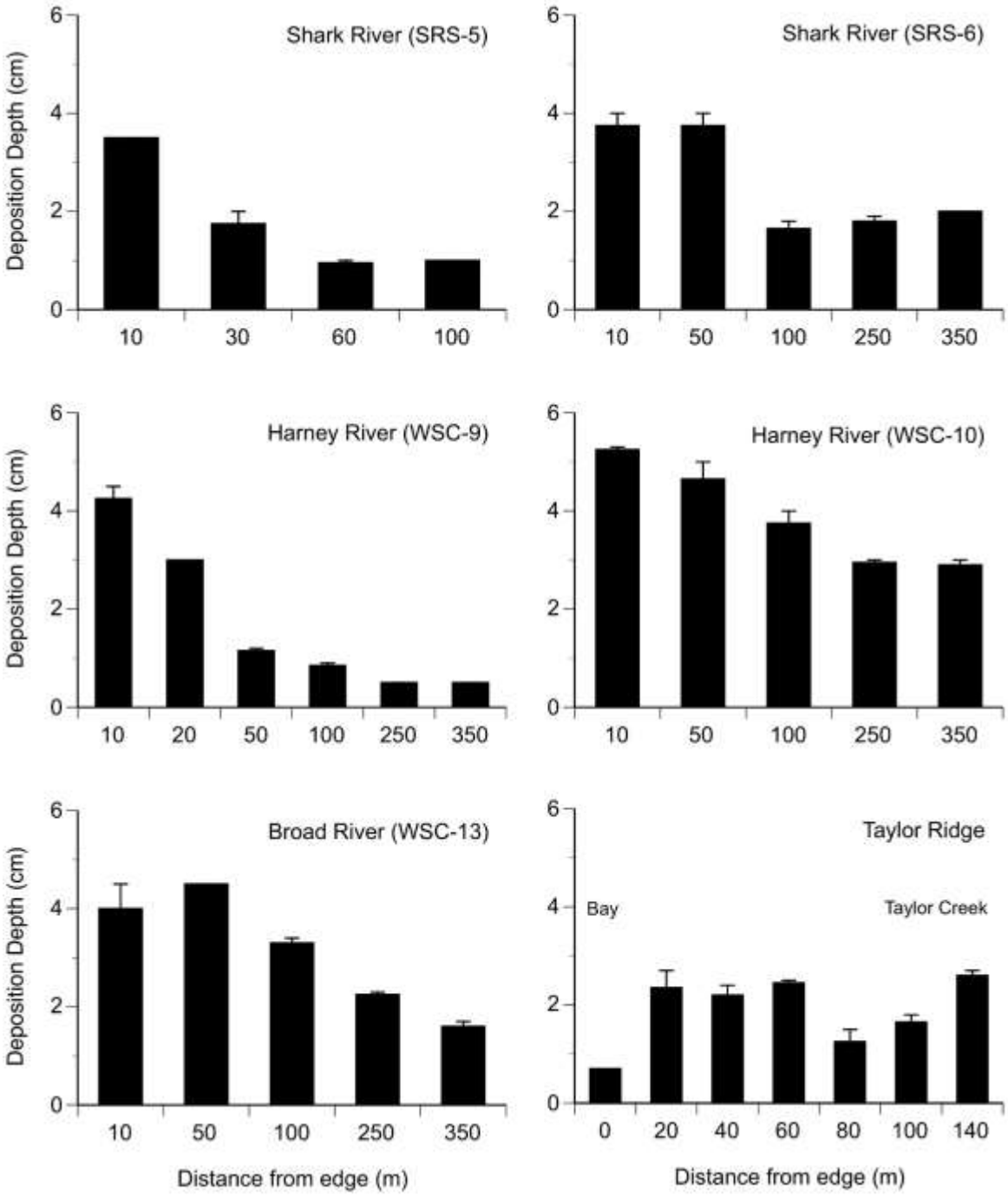

Figure 10. Mean (±1 SE) bulk density and organic matter content of storm sediments and surface soils in mangrove sites of the Florida Coastal Everglades.

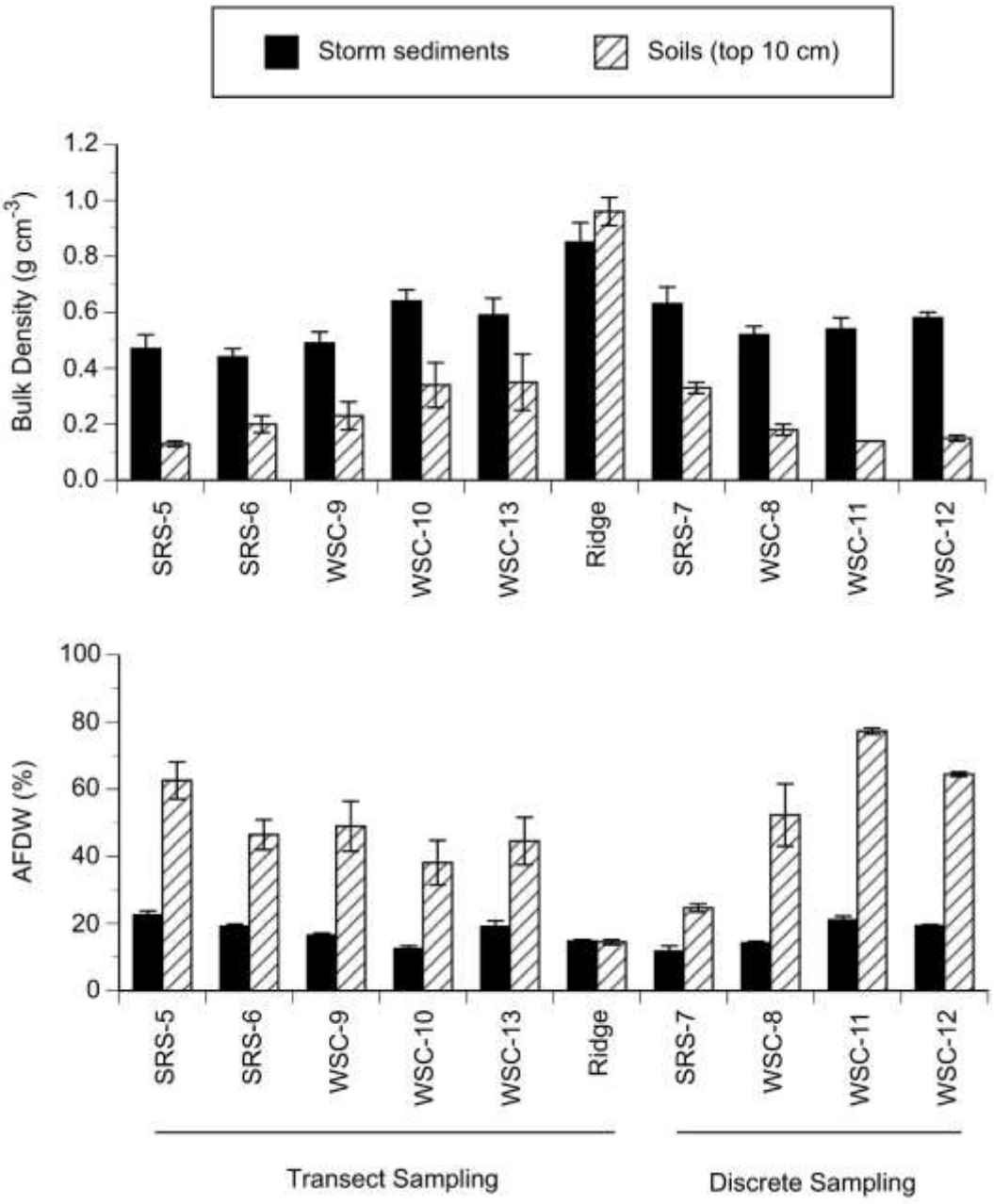

Figure 11. Mean (±1 SE) total nitrogen and phosphorus in storm sediments and surface soils at mangrove sites sampled in transects and discrete sampling points in the Florida Coastal Everglades after the passage of Hurricane Irma on September 10, 2017.

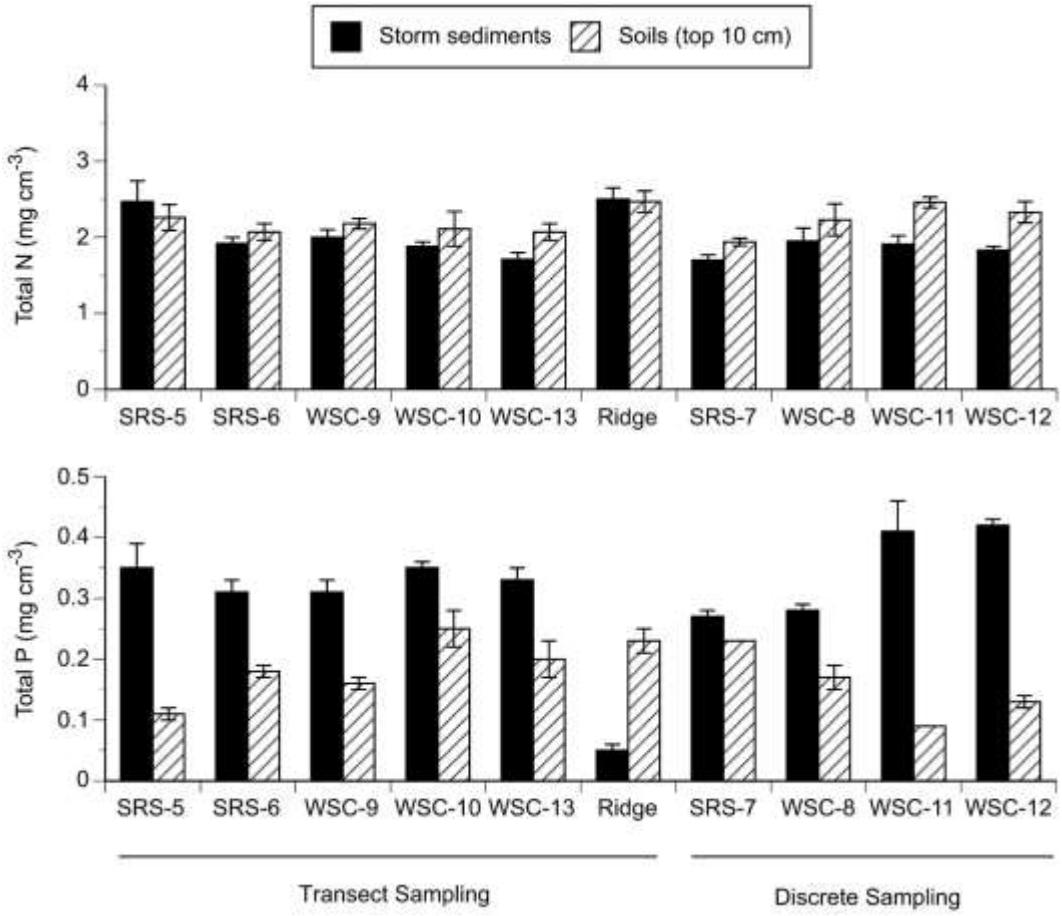

Figure 12. Tree defoliation and canopy openness in mangroves sites sampled in the Florida Coastal Everglades after the passage of Hurricane Irma on September 10, 2017.

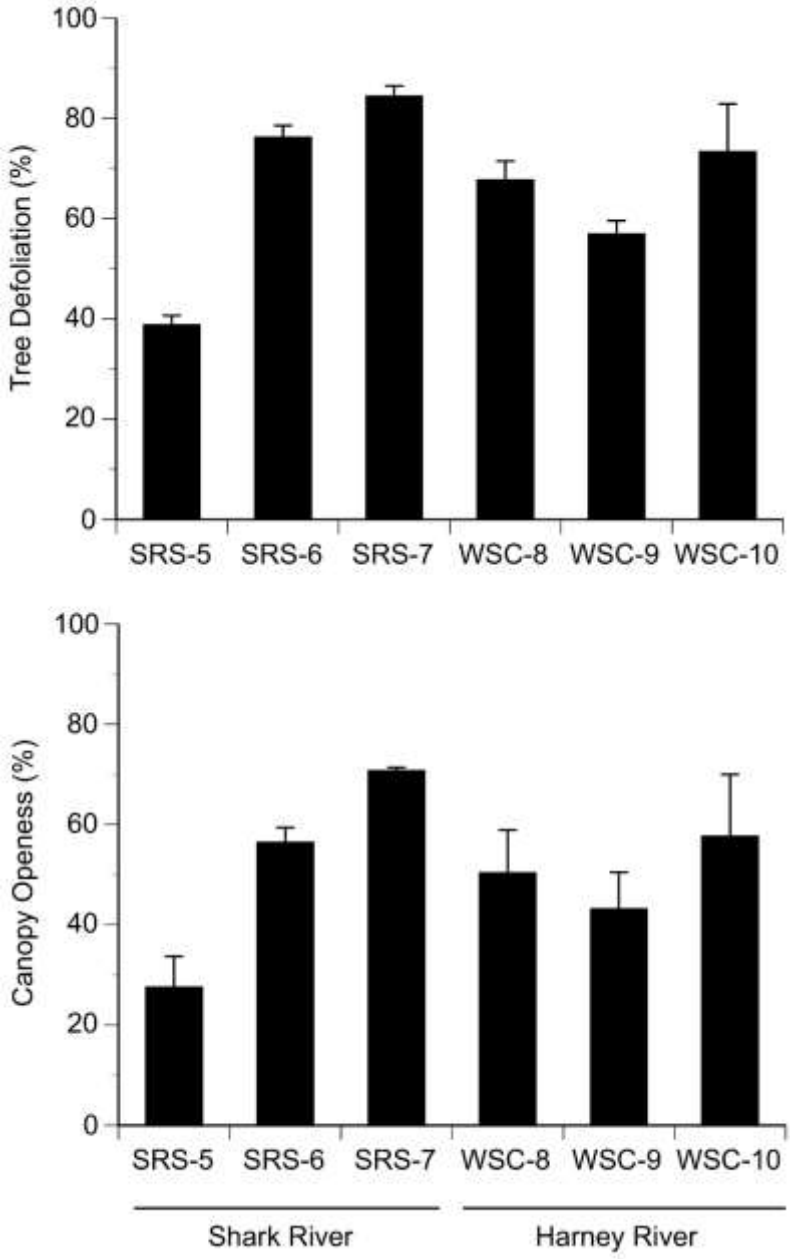

Figure 13. Variation in standing aboveground (AG) biomass in mangroves sites sampled in the Florida Coastal Everglades after the passage of Hurricane Irma on September 10, 2017.

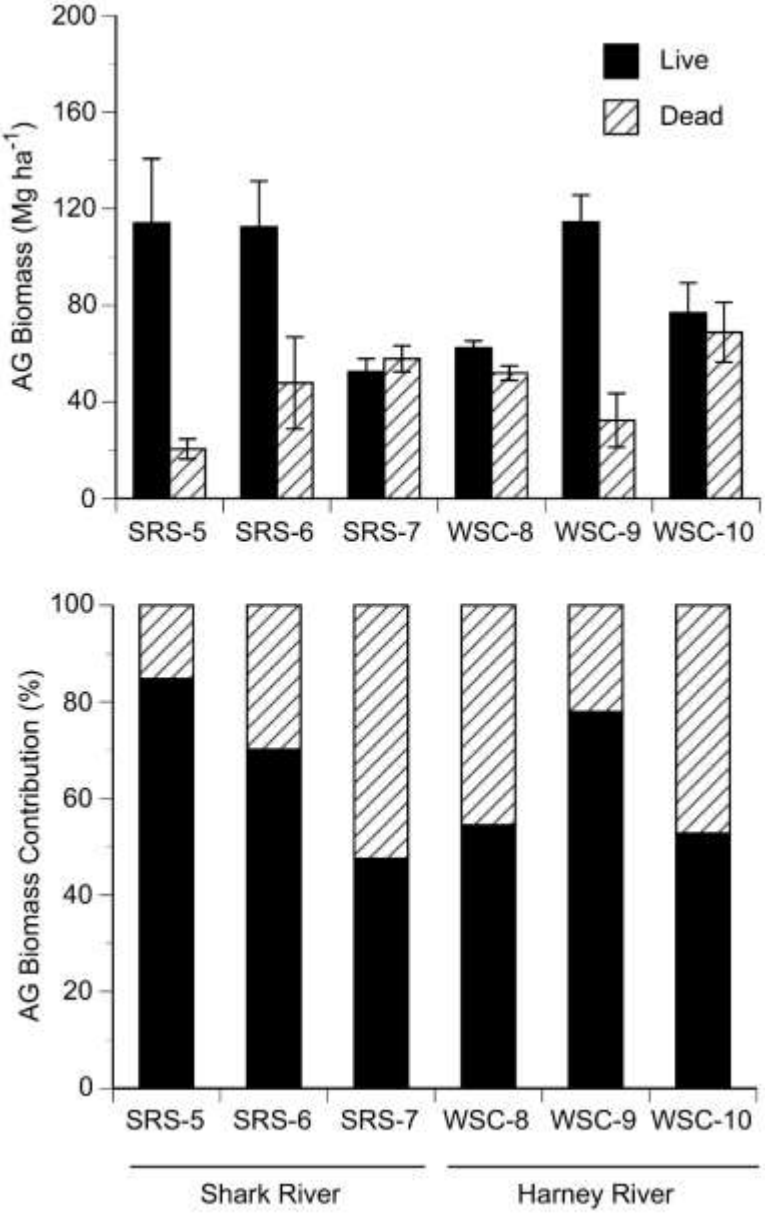

Figure 14. Mean (±1 SE) total (coarse and fine) woody debris in mangrove sites sampled in the Florida Coastal Everglades after the passage of Hurricane Irma on September 10, 2017.

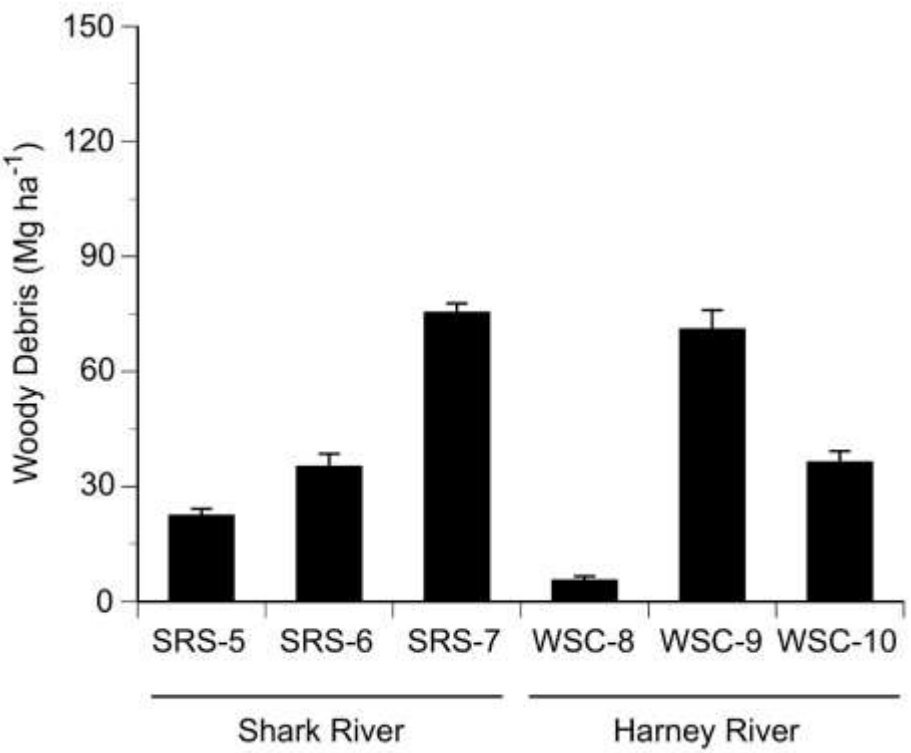

Figure 15. Variation in tree mortality and density of dead trees in mangrove sites sampled in the Florida Coastal Everglades after the passage of Hurricane Irma on September 10, 2017.

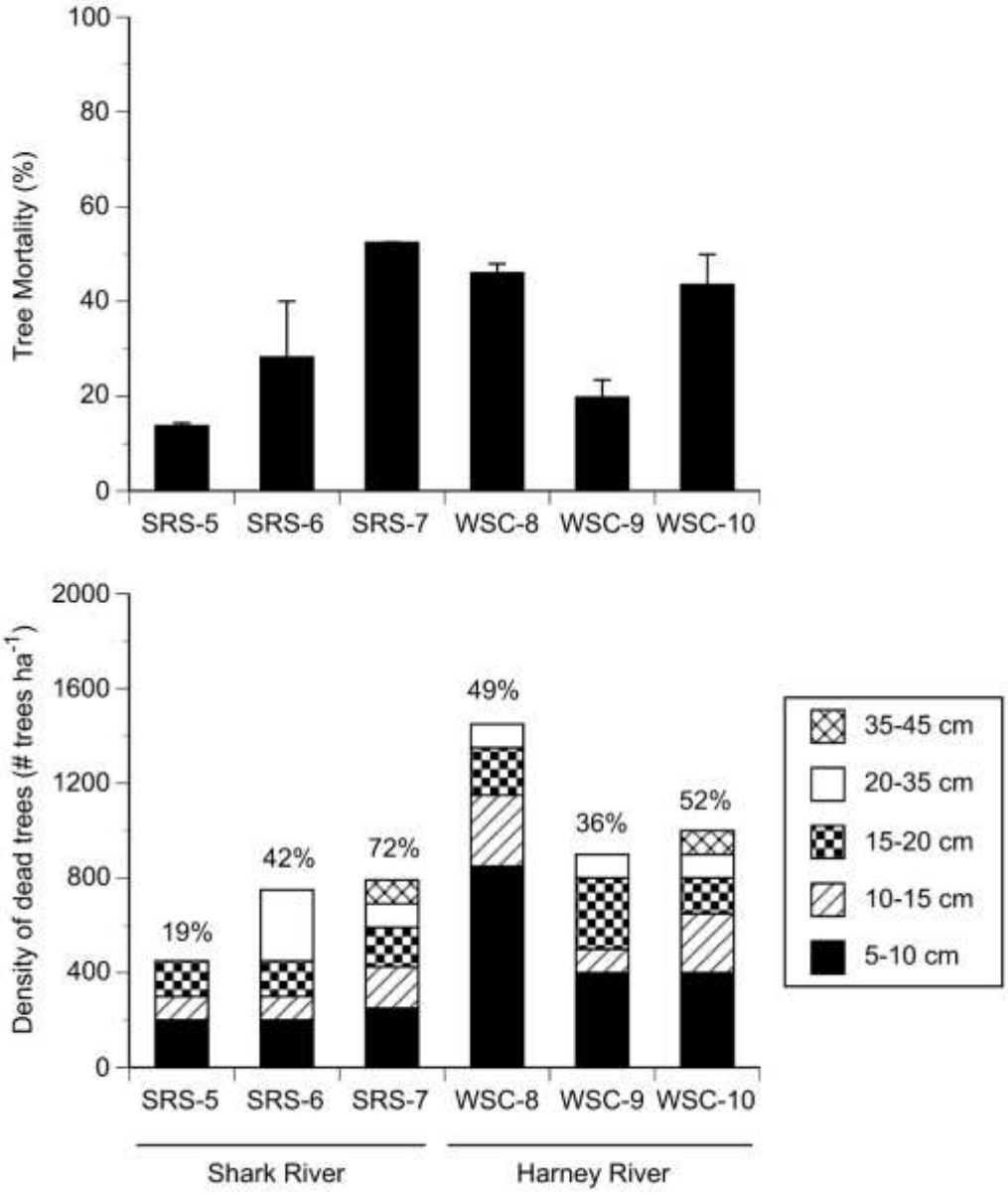

Figure 16. Total phosphorus concentrations in monthly water samples from Shark River Slough (top – marsh sites; bottom – estuary sites) showing post-Hurricane Irma spikes, particularly in the coastal zone.

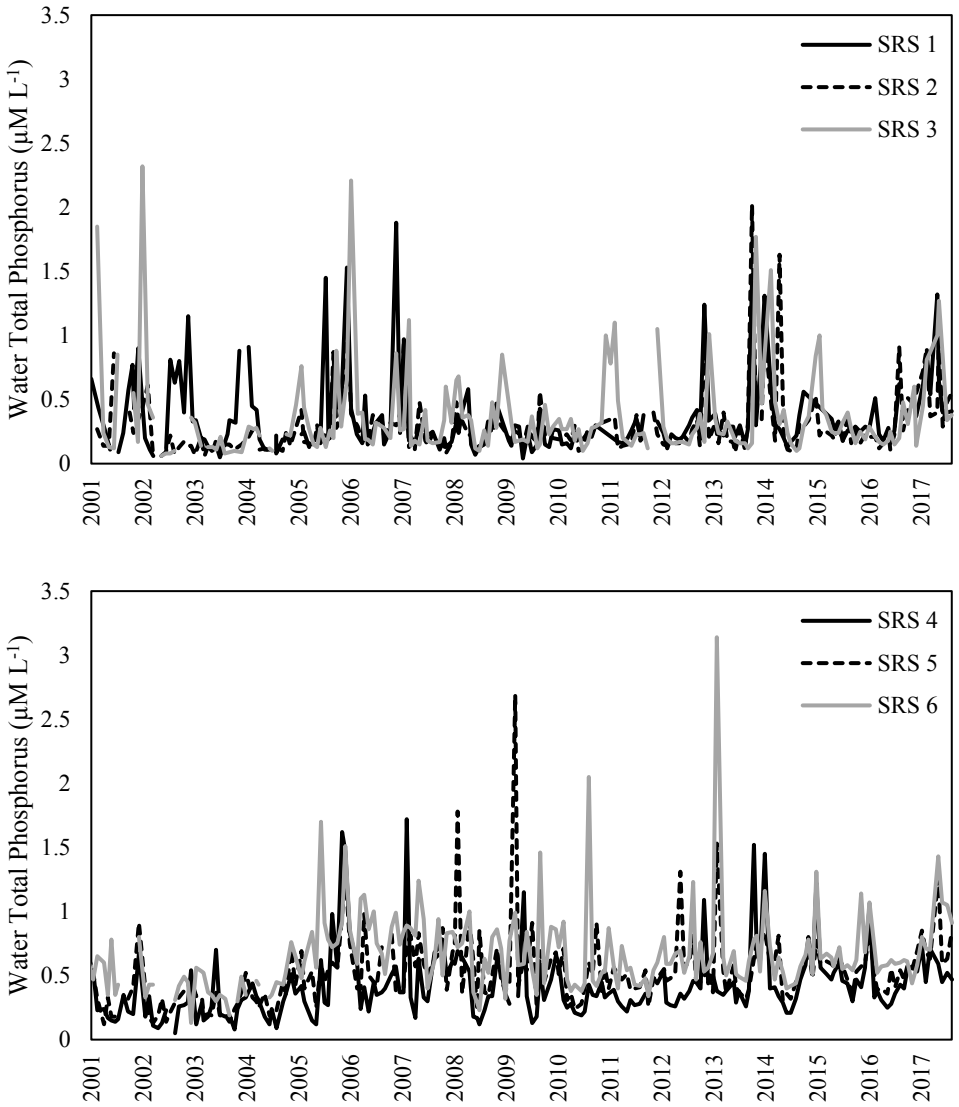

Figure 17. Dissolved organic carbon concentrations in monthly water samples from Shark River Slough (top – marsh sites; bottom – estuary sites) showing post-Hurricane Irma spikes, particularly in the coastal zone.

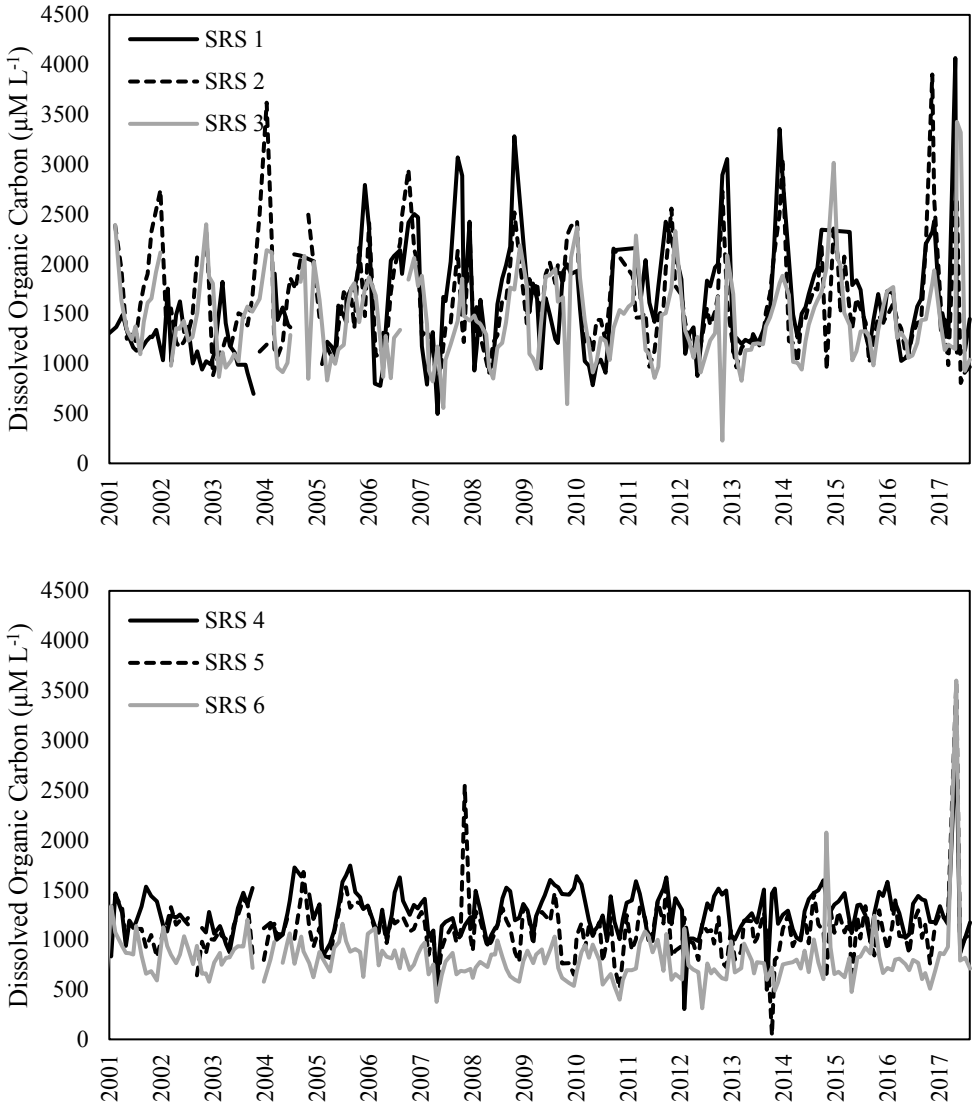

Figure 18. Root decomposition rates after 190 d of incubation in surface (0-20 cm) and subsurface soils (20-40 cm) along an upstream-downstream gradient in FCE mangrove sites (SRS-4, 5, 6, and 7).

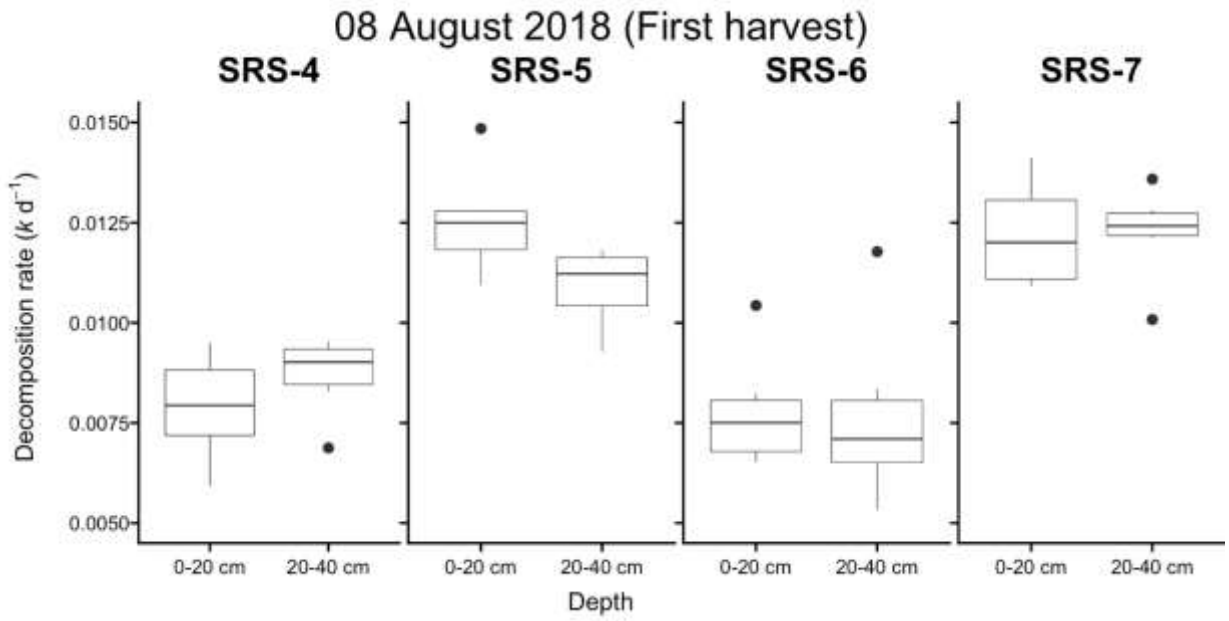

Figure 19. Environmental conditions in the Shark River for the 10 days surrounding Hurricane Irma (landfall at 15:00 UTC on 9/10/2017, red dotted line). Shading in all 3 panels shows the 67-hr hurricane window denoted by rapidly changing environmental conditions associated with the storm. a) Modeled barometric pressures for the upper and lower rivers showing a rapid decline with the approaching storm. b) River stage in the lower river illustrating the drop in water levels (anti-surge), and spike with storm surge. c) Stage in the upper river increasing with heavy rainfall.

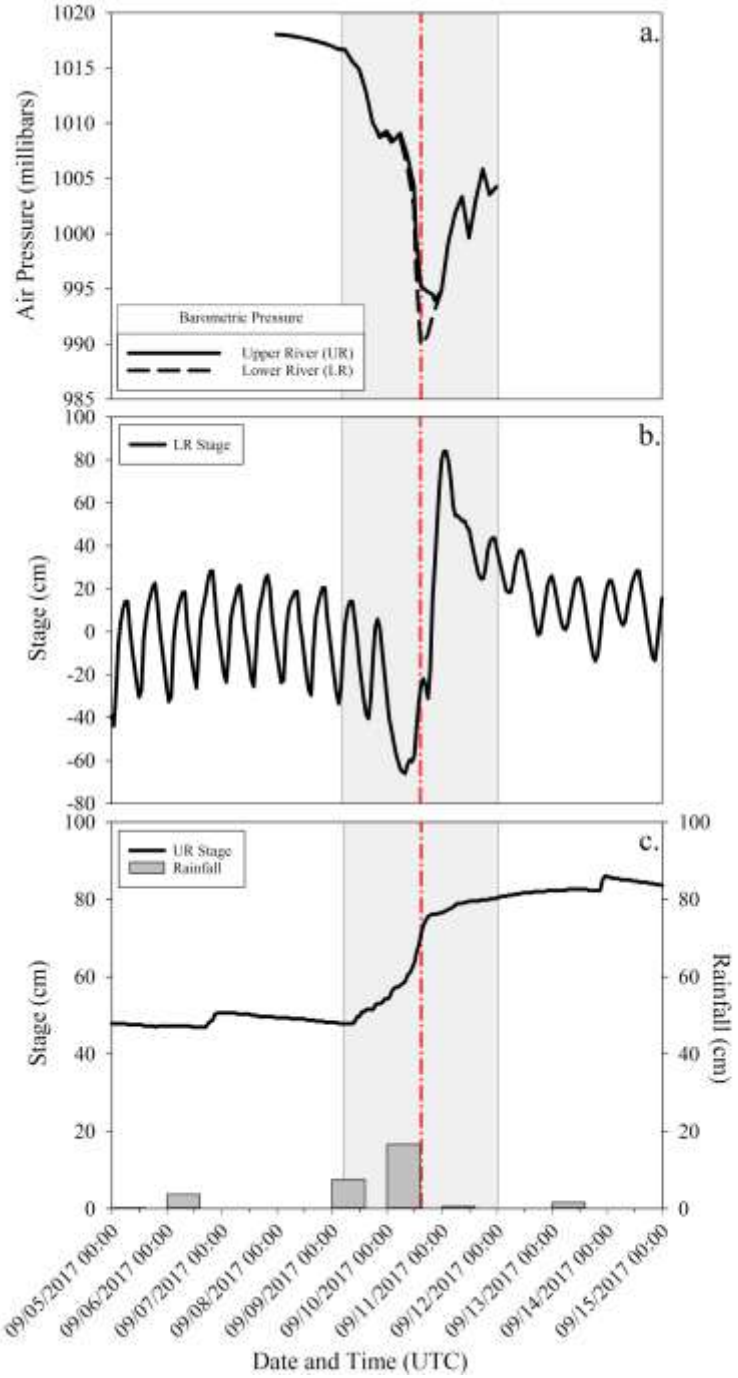

Figure 20. Examples of raw acoustic receiver detection data for three tagged Common Snook (*Centropomus undecimalis*) in the two weeks leading up to and following Hurricane Irma (indicated by vertical dotted line), showing three observed patterns of movement: a) fish that moved from the upper river to Tarpon Bay, b) fish that moved from the upper river and were last detected on downstream most receivers of the acoustic array, possibly depicting an exit of the river to the coast, and c) fish that did not move and continued to be detected in the upper river. The fish depicted in panel a) was not re-detected as of receiver downloads in June of 2018, indicating a possible relocation outside the system or mortality. The fish in panel b) was re-detected on a coastal receiver on 12/14/2018 (beyond period depicted here), corroborating that it exited the system and had not returned to the river post-hurricane.

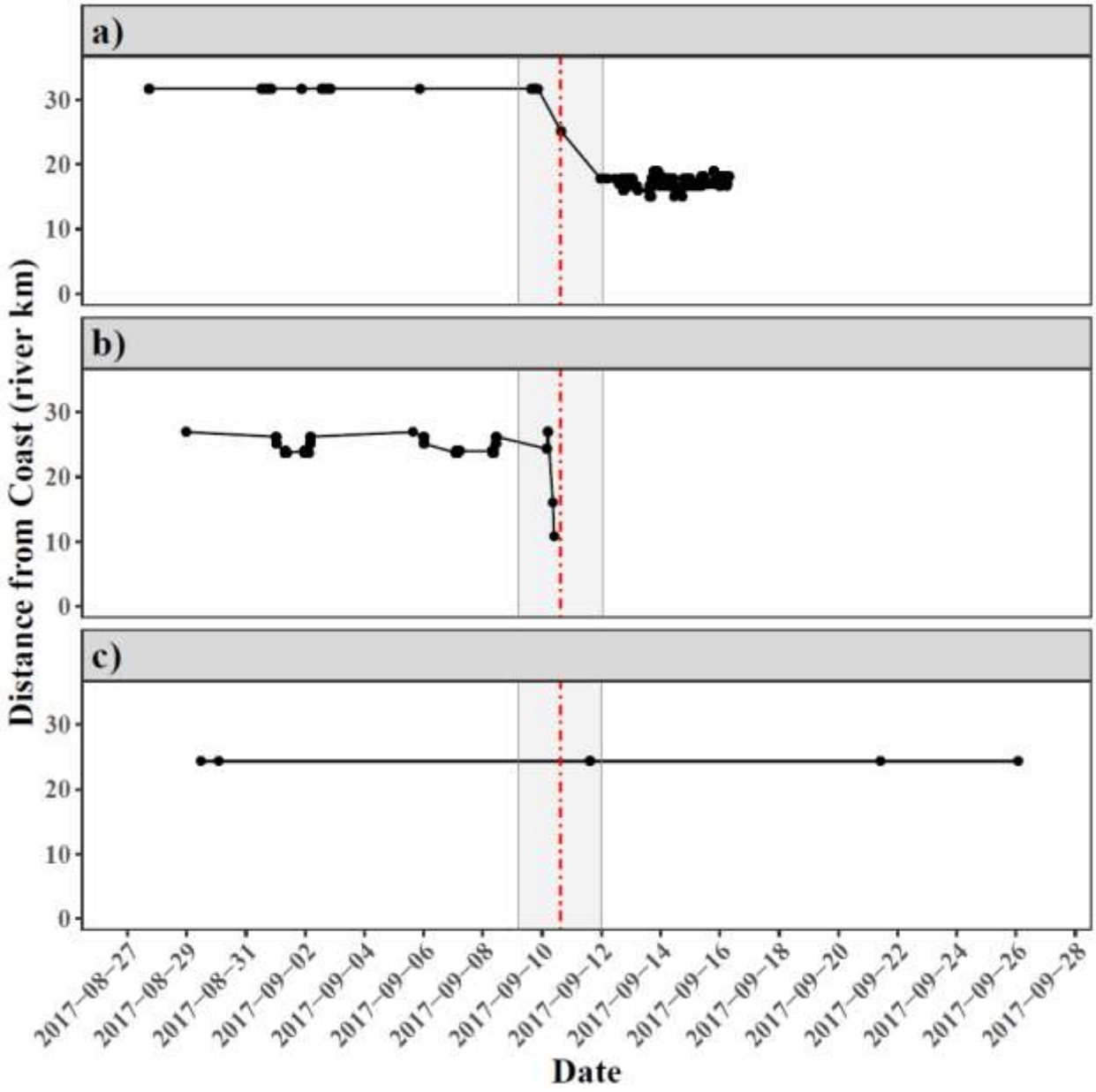

Figure 21. Hourly proportion of juvenile Bull Sharks (*Carcharhinus leucas*) within our tagged sample that were detected within an acoustic telemetry array in the Shark River. Red dotted line denotes the estimated time Hurricane Irma was reported to be approximately 60 km from the Shark River mainstem at 15:00 UTC 10 September 2017.